

EPR Characterization of Ferroelectric Ceramics (Sb, Cu)-Doped BaTiO₃

Said Daoudi^{1,*}, Lahcen Bejjit¹, Mustapha Haddad¹, El Mostapha Yahiaoui¹,
Lahcen Bih², Faouzi Bensamka³, Ahmed Outzourhit³

¹Laboratoire de Spectrométrie des Matériaux et Archéomatériaux (LASMAR - URAC11), Faculté des Sciences, Université Moulay Ismail, B.P. Zitoune, Meknès, Morocco

²Equipe physico-chimie de la matière condensée, Faculté des Sciences, Université Moulay Ismail, B.P. Zitoune, Meknès, Morocco

³Laboratoire des Sciences des Matériaux, Faculté des Sciences Semlalia, BP, Université Cadi Ayyad, Marrakech, Morocco

Abstract This work presents the results of an EPR study of BaTiO₃ (BTO) ferroelectric ceramics pure and doped with antimony and copper. This study revealed the nature of the defects created in pure BTO and those generated by the effect of dopant. The computer simulation of the EPR spectra showed that these spectra are composed of several signals related with the presence of the paramagnetic centers in the doped and undoped BTO structure. These centers are identified, by determining their EPR parameters, as defects V'_{Ba} , V''_{O} , V''''_{Ti} and Ba.

Keywords Ceramics, Electron paramagnetic resonance (EPR), Structural defects

1. Introduction

Perovskite-type BaTiO₃ ceramics have many applications in various domains, especially in electronics and telecommunications because of their piezoelectric, pyroelectric and ferroelectric properties [1-7]. To improve the properties of these materials and adapt them to specific applications, several doping elements have been added to BaTiO₃ structure [8-17]. The obtained ferroelectric ceramics have been characterized by different method [18-20].

In last years, many works have focused on the defects created by doped BTO using electron paramagnetic resonance (EPR), a powerful tool for identifying paramagnetic elements and crystalline defects. Kolodiazhnyi and Petric [21], Dunbar et al. [22] and Castro et al. [23] have associated EPR singlet, with g values between 1.973 and 1.974, to the singly ionized barium vacancy (V'_{Ba}), and room temperature investigations [21] revealed the same signal in both of doped and undoped BaTiO₃, after oxidation of reduced ceramics in air. The g = 2.004 EPR signal has been attributed to the titanium vacancy with unpaired electron spin, i.e. V'_{Ti} or V''''_{Ti} . Recently, Lu et al. [16, 17] have identified several paramagnetic point defects in Pr-doped BaTiO₃ and La, Tb co-doped BaTiO₃ ceramics. In the first material the authors have associated EPR singlet, with g = 2.002 to the singly ionized Ti-vacancy defects, the signal at g= 1.932 to Ti^{3+} ($3d^1$) and the signal at g= 1.974 to Ba

vacancies. In the second material the EPR signals at g = 2.004 and g=1.974 have been attributed to $V_{(Ti)}$ and $V_{(Ba)}$ defects respectively.

In this paper, we have studied the effect of antimony and copper dopants on the BaTiO₃ (BTO) composition. Using EPR technique, we tried to identify ionized barium, titanium and oxygen vacancies produced in doped BaTiO₃ lattice by Sb and Cu elements.

2. Experimental Procedures

2.1. Samples Preparation

Perovskite ceramics of BaTiO₃ type were prepared by the hydrothermal method [24]; Barium hydroxide Ba(OH)₂ is prepared by dissolving barium oxide BaO in distilled water. A mixture of Ba(OH)₂, TiO₂, Sb⁵⁺ or Cu²⁺ aqueous solution was introduced in an autoclave. The media is rendered alkaline by adding sodium hydroxide NaOH. Then, it is heated to 140°C and maintained at this temperature for 14 hours. The obtained product is filtered, washed to eliminate Na⁺ ions and dried at 100°C.

2.2. EPR and XRD Measurements

The EPR spectra X-band (9.5 GHz) were recorded at room temperature on powder samples, using a Bruker spectrometer. The numerical simulation of the experimental spectra was carried out by developing a computational program well adapted to the nature of the paramagnetic centers studied in this work.

The X-ray diffraction (XRD) studies were performed in a set-up equipped with a Siemens M386-X-A3 goniometer

* Corresponding author:

daoudi.said@gmail.com (Said Daoudi)

Published online at <http://journal.sapub.org/materials>

Copyright © 2017 Scientific & Academic Publishing. All Rights Reserved

using the CuK α radiation.

3. Results and Discussions

3.1. Structural Properties

Barium titanate (BaTiO₃) ceramics were analyzed by X-ray diffraction (XRD) [24]. Figure 1 shows typical XRD diagrams of the dried BaTiO₃ powders prepared at two different reactor temperatures at 120 and 140°C. These diagrams show the presence of the characteristic peaks of the cubic phase of BaTiO₃. A secondary phase identified as anatase TiO₂ is also observed. One can notice that the amount of these impurity phase decreases as the reactor temperature is increased from 120 to 140°C.

We can conclude, from these results, that BaTiO₃ starts to form at low temperature 120°C. The crystallinity of the obtained BaTiO₃ improves when the reaction temperature is increased to 140°C since the corresponding XRD peaks became more intense and narrower.

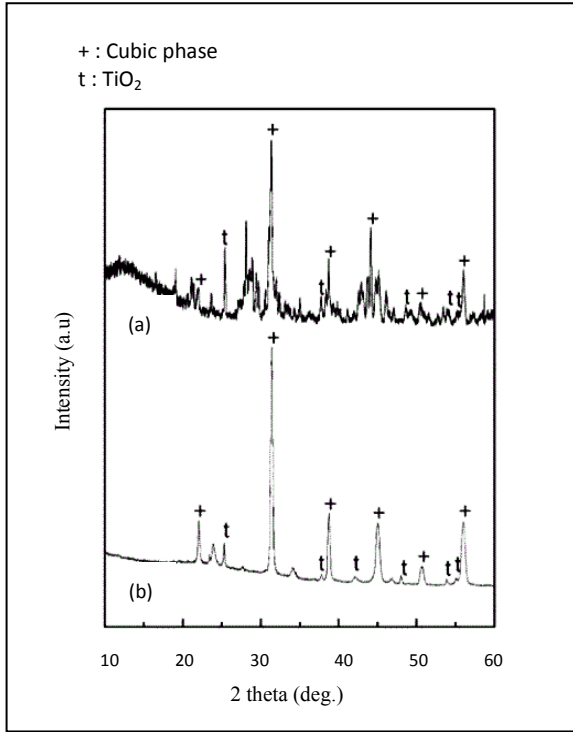


Figure 1. XRD patterns of untreated BaTiO₃ powders prepared at: (a) 120°C; and (b) 140°C

3.2. EPR Results

For each sample we give the experimental and the calculated spectrum. The numerical simulation of the experimental spectra was carried out using a spin Hamiltonian composed of electronic Zeeman and hyperfine terms:

$$\hat{H} = \beta SgH + SAI$$

H is the magnetic field strength, A is the hyperfine constant, S and I are electronic and magnetic spin

respectively. g is the gyromagnetic factor calculated by the relationship $h\nu_0 = g\beta H$, where h is the plank constant ($6,626 \times 10^{-34}$ J s), ν_0 is the microwave frequency and β is the Bohr magnetron (9.262×10^{-24} J/T).

3.2.1. BaTiO₃ Undoped

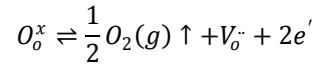
The EPR spectrum from the undoped BaTiO₃ sample is shown in figure 2. The calculated spectrum allowed us to identify several types of paramagnetic centers (Table 1). The hyperfine structure with six lines is due to Mn²⁺ (3d⁵, ⁶S_{5/2}) and the signal with g = 2,000 (relatively high intensity) is attributed to the Fe³⁺ (3d⁵, ⁶S_{5/2}), both of these elements are the main impurities associated with titanium in the BaTiO₃ [11, 16, 21, 23]. The low intensity signals at g = 2.004 and g = 1.974 are attributed respectively to titanium vacancies (V_{Ti}'''') [9] and barium vacancies (V_{Ba}') [16, 21, 23]. The low intensities of these signals can be associated with small quantities of V_{Ba}' and V_{Ti}'''' in the undoped BaTiO₃ ceramics [21, 25].

Table 1. EPR parameters deduced from BaTiO₃ spectrum simulations

Parameters	Paramagnetic centers			
	V_{Ti}''''	V_{Ba}'	Fe ³⁺	Mn ²⁺ (central line)
g	2.004± 0.001	1.974± 0.001	2.000± 0.001	2.0024± 0.001
A	-	-	-	83
Linewidth ΔH (G)	35	15	35	4

3.2.2. EPR Spectrum of Sb-doped BaTiO₃

Figure 3 shows an experimental and calculated EPR spectrum of BaTiO₃ doped with 0.3% antimony. In addition to signals previously detected in the non-doped BaTiO₃ spectrum (Table 1), we observe a hyperfine structure with 4 lines around $g_{\parallel} = 2.38$ and $g_{\perp} = 2.063$ [26]. This hyperfine structure corresponds probably to the Ba⁺ center (Ba²⁺ + 1e⁻ → Ba⁺) which is a reduced ion by the electrons coming from oxygen vacancies according to the following equation [26, 27]:



As it is well known, barium has two isotopes, ¹³⁵Ba and ¹³⁷Ba, which have the same nuclear spin (I = 3/2), and with natural abundances of 6.59% and 11.32%, respectively. This is what justifies that the EPR spectra show a hyperfine structure with 4 lines which are not clearly distinguished. On the other hand, comparing the spectra from undoped BaTiO₃ and Sb-doped BaTiO₃, the signal related to the barium vacancies increases significantly. This could be give information about the site occupied by antimony. In fact, the increasing intensity of this signal indicates that the sites associated to barium vacancies (V_{Ba}') are created with Sb-doping of BTO. This could be explained by the fact that the antimony ion introduces the BTO network by occupying the Ti⁴⁺ site. Indeed, according to the ionic radius of the elements existing in the structure (Table 2), we see that the

antimony Sb^{5+} can occupy the Ti^{4+} site. The mechanism of the formation of these barium vacancies is represented by the following equations [23]:

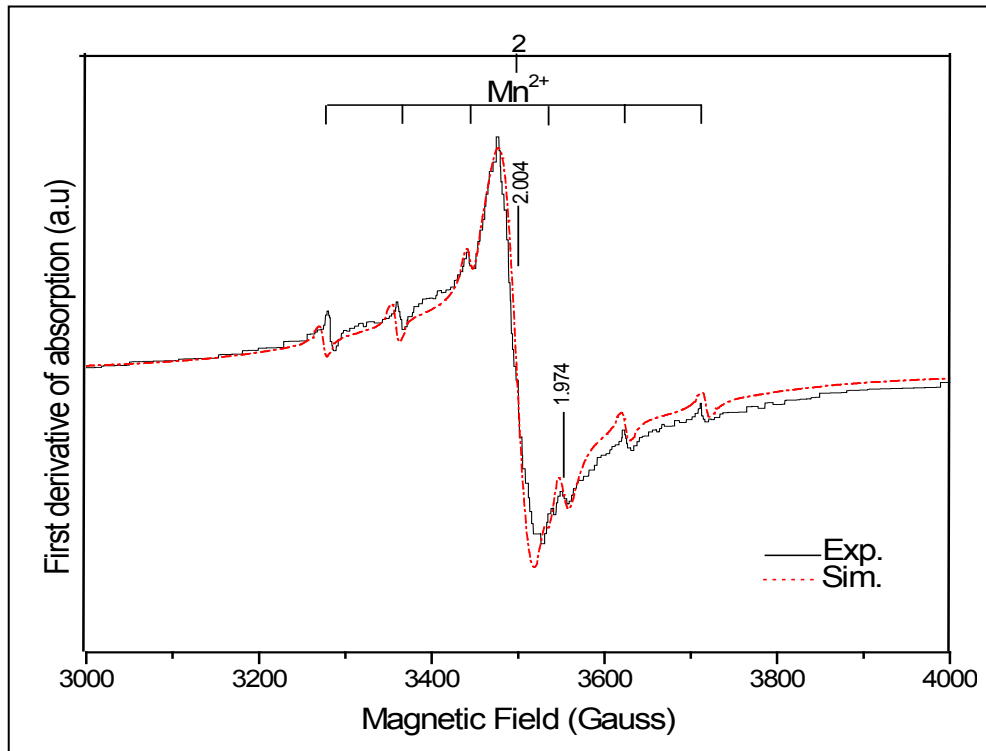
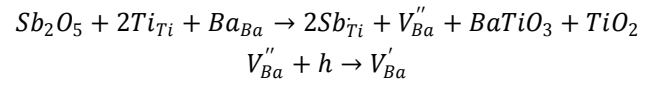


Figure 2. Experimental and calculated EPR spectrum of BaTiO₃

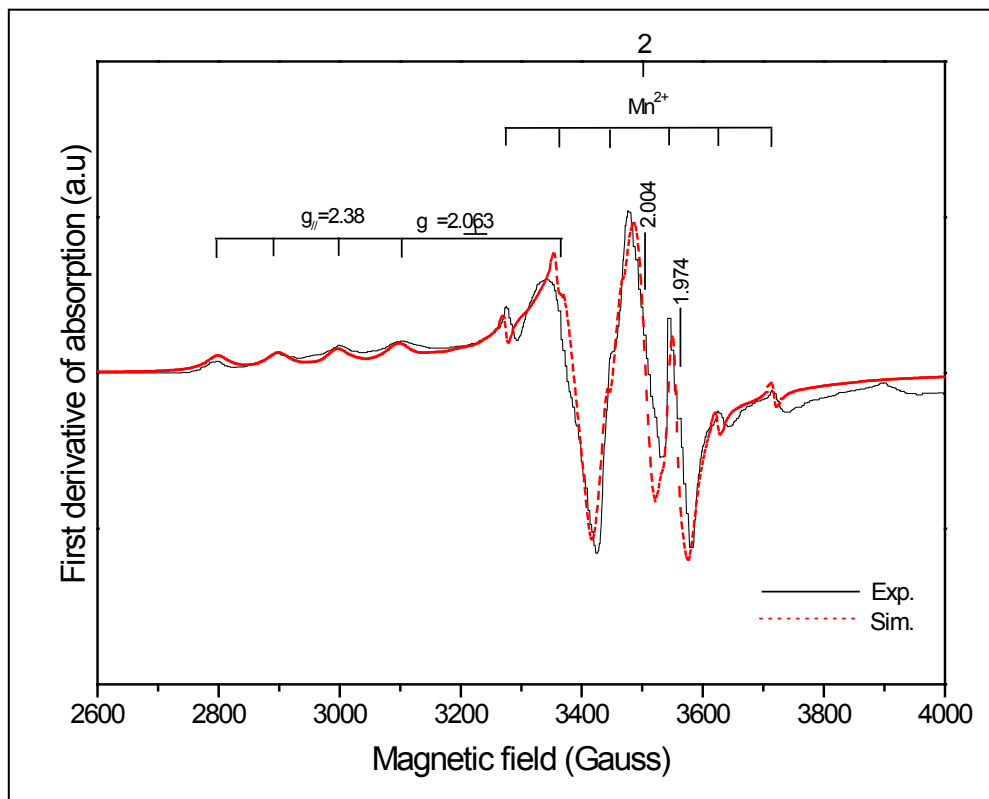


Figure 3. Experimental and calculated EPR spectrum of 0.3% Sb-doped BaTiO₃

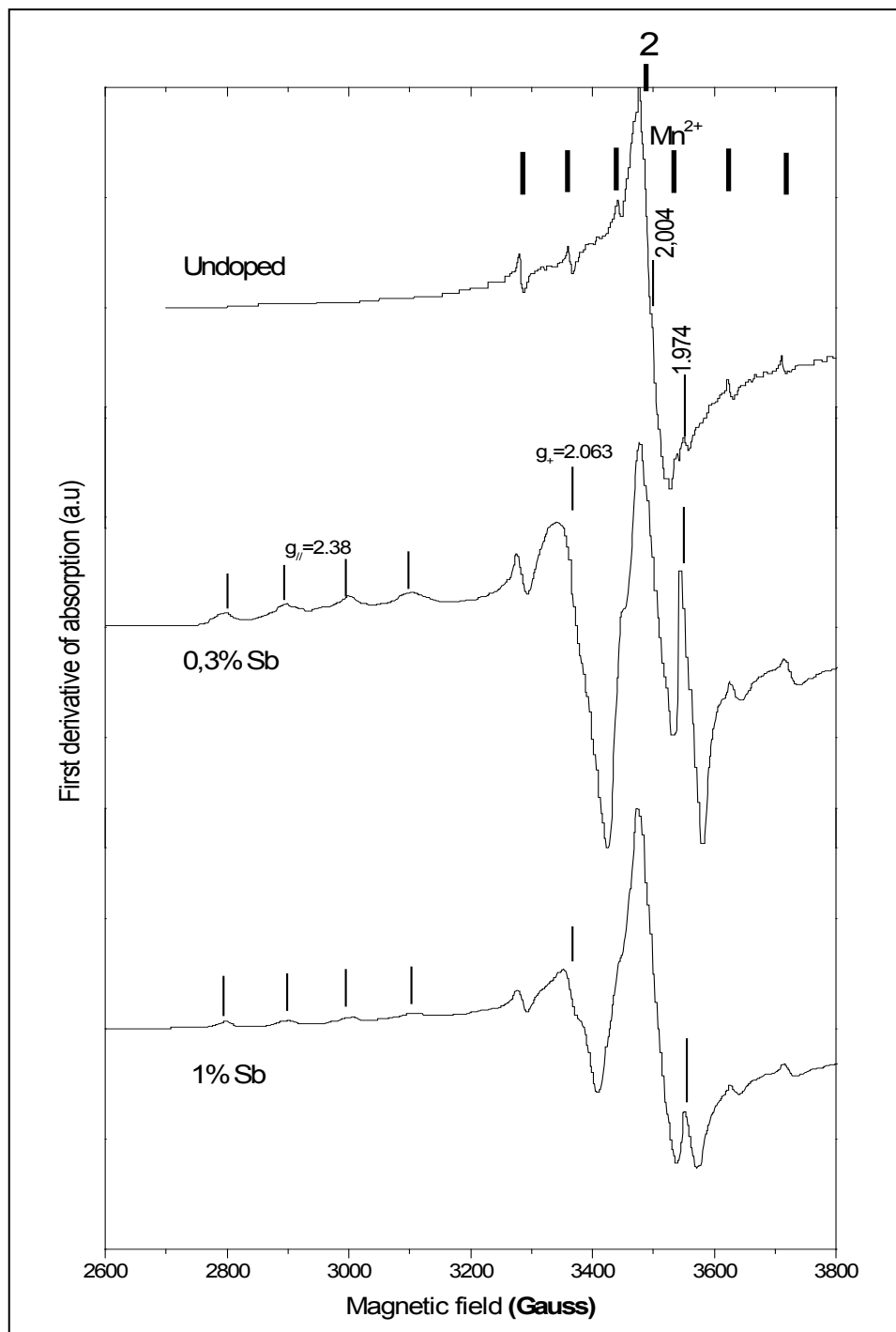


Figure 4. EPR Spectra of undoped and Sb-doped BaTiO₃

It is worth to note that the V'_{Ba} species produced by the double ionization of V''_{Ba} are paramagnetic [23].

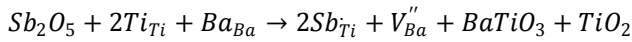
Table 2. Radius values of some ionic elements

Ions	Ti ³⁺	Ti ⁴⁺	Sb ⁵⁺	Ba ²⁺	Cu ²⁺
Size (Å)	0,74	0,61	0,62	1,35	0,92

In order to study the effect of doping content on the shape of the EPR spectrum and the created vacancies, the EPR spectra of the undoped, 0.3% Sb-doped and 1% Sb-doped

BaTiO₃ are presented together (Figure 4). By normalizing and comparing the spectra of 0.3% Sb and 1% Sb, we can observe two opposite effects when the concentration of the Sb increases: (i) the intensity of signals associated to V'_{Ba} and Ba^+ centers decreases, (ii) the intensity of V''_{Ti} center increases. This means that the doping content has a significant effect on the nature of the created paramagnetic centers in the BaTiO₃ structure. These results are in good agreement with the mechanism proposed by Castro *et al.* [23], to describe the creating defects in Sb-doped BaTiO₃:

-For the low rate 0.3% Sb:



-For high rate 1% Sb:



3.2.3. EPR Spectra Cu-doped BaTiO₃

EPR spectra are recorded for 0.3% and 1% Cu-doped BaTiO₃. All the identified EPR signals in undoped BTO are present in doped samples. However, the Cu-doping induces the appearance of new signals. The calculated spectrum for 1% Cu-doped (Figure 5) allowed us to distinguish several lines, three hyperfine structures around ($g_{\parallel}=2.35$ and $g_{\perp}=2.096$), ($g_{\parallel}=2.3$ et $g_{\perp}=2.027$) and ($g_{\parallel}=2.38$ and $g_{\perp}=2.063$); the two first hyperfine structures are attributed to Cu²⁺ ions in two different sites [28] and the third one is attributed to Ba⁺ ions. The weak line at $g = 1.963$ is attributed to oxygen vacancies [23].

We retain as result here that the Cu doping causes the creation of oxygen vacancies. Indeed, according to the table 1 and to the mechanism of defects ($BaO + CuO \rightarrow Ba_{Ba}^x + Cu_{Ti}'' + V_o^{\cdot} + 2O_o^x$) established by Langhammer et al. [28], the copper can occupy titanium site. In the other hand, the comparison of EPR spectra from 0.3% and 1% Cu-doped

BaTiO₃ samples (Figure 6) revealed that as copper content increases, Cu²⁺ signals increase and the intensity of the signal ($g = 1.963$) associated with V_{Ba}'' increases.

The creation of V_{Ba}'' defects which can be described by the equation $Mn_2O_3 \rightarrow Mn_{Ba} + V_{Ba}'' + 3O_o$ and the weakness of Mn²⁺ signal intensity could be explained by the process of oxidation-reduction of manganese present in BaTiO₃ as impurity, according to the following reaction:



4. Conclusions

The Sb-BTO and Cu-BTO ceramics are prepared by the hydrothermal method and are studied by EPR. Their experimental and simulated spectra showed the presence of several paramagnetic centers, namely V_{Ba}' , V_{Ti}'''' , V_o^{\cdot} and Ba⁺. The defects identified depend on the nature of the dopant; those identified in Sb-BTO are V_{Ba}' , V_{Ti}'''' and Ba⁺ and those contained in Cu-BTO are V_{Ba}' , V_{Ti}'' , V_o^{\cdot} , Ba⁺ and Cu²⁺. It's also found in Sb-BaTiO₃ ceramics that the intensity of V_{Ba}' and Ba⁺ centers decreases and the intensity of V_{Ti}'''' center increases with Sb doping of BaTiO₃.

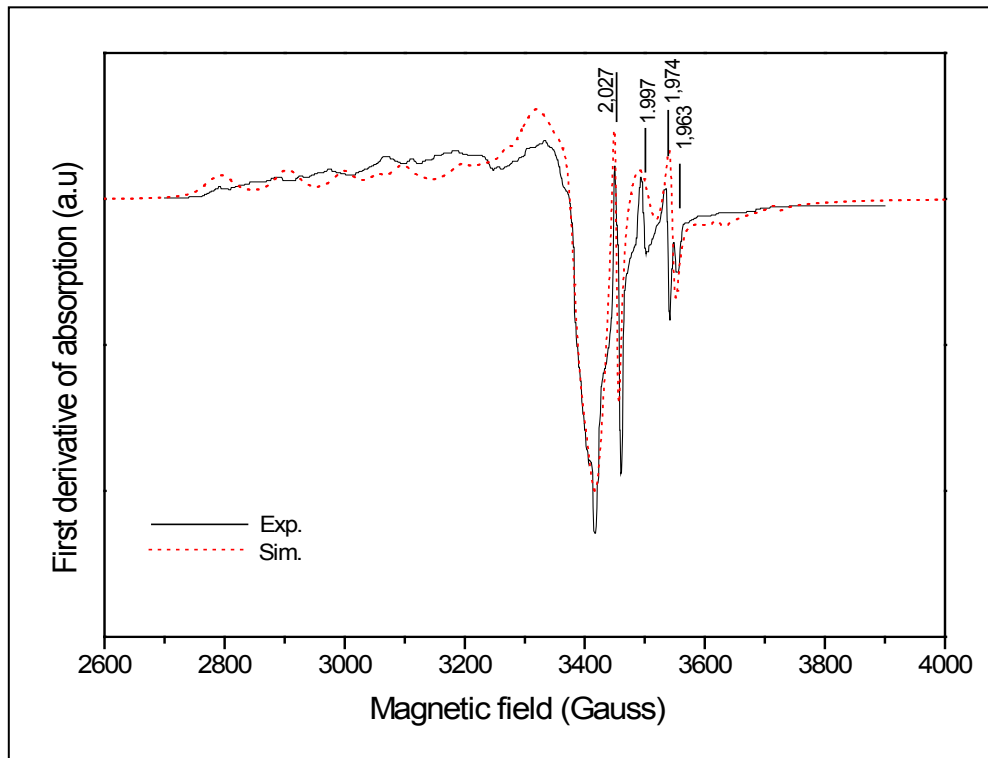


Figure 5. Experimental and calculated EPR spectrum of 1% Cu-doped BaTiO₃

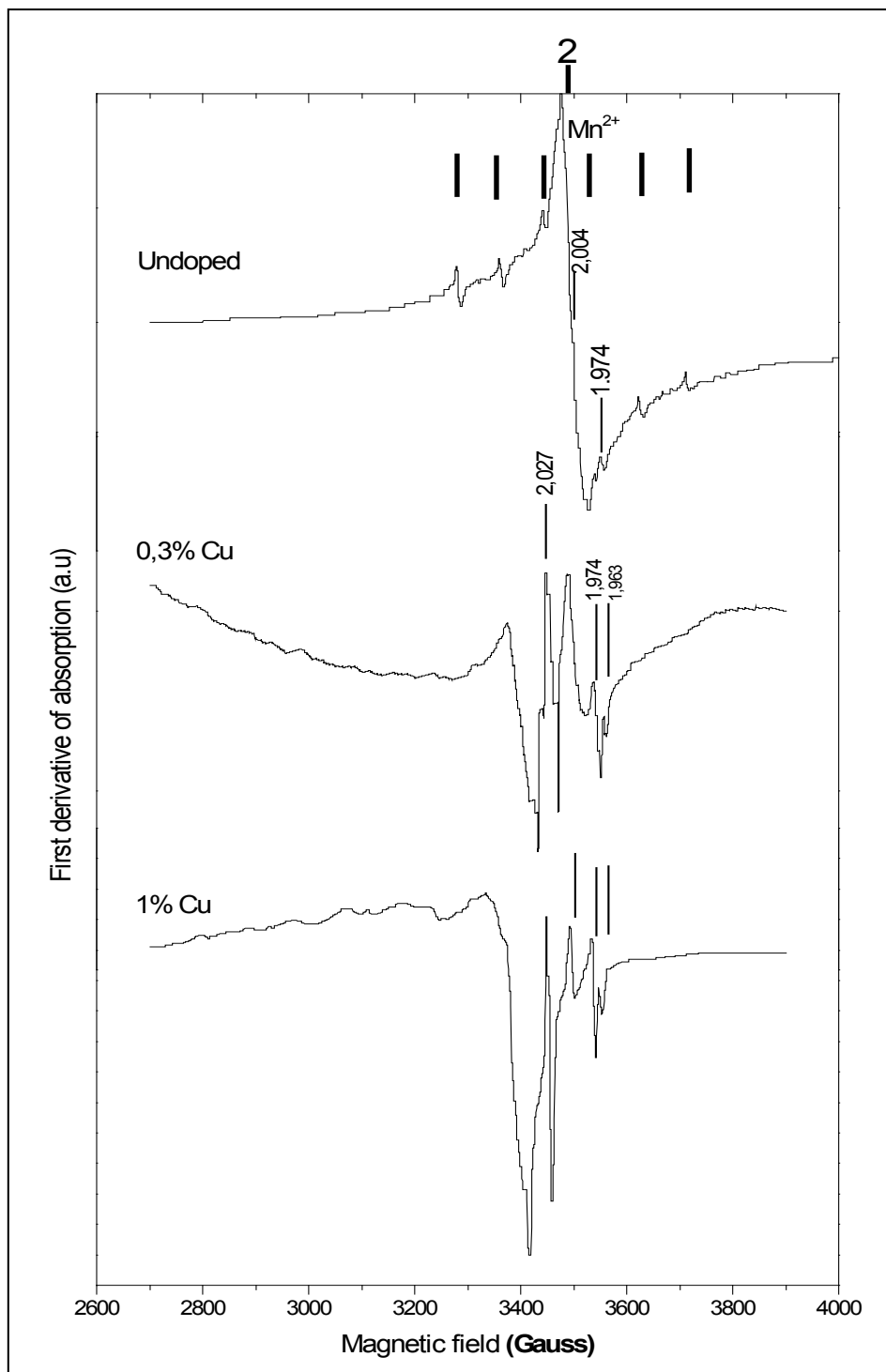


Figure 6. EPR spectra of undoped and Cu-doped BaTiO₃

REFERENCES

- [1] H. Gong, X. Wang, S. Zhang and L. Li, Synergistic effect of rare-earth elements on the dielectric properties and reliability of BaTiO₃-based ceramics for multilayer ceramic capacitors, *Materials Research Bulletin*, 73 (2016), 233-239.
- [2] Burcu Ertuğ, The Overview of The Electrical Properties of Barium Titanate, *American Journal of Engineering Research (AJER)*, 02 (08) (2013) 01-07.
- [3] Y. Mizuno, T. Hagiwara and H. Kishi, Microstructural design of dielectrics for Ni-MLCC with ultra-thin active layers, *J. of the Ceramic Society of Japan*, 115 (2007) 360-364.
- [4] N. Sareecha, W.A. Shah, M.A. Rehman, M.L. Mirza, M.S. Awan, Electrical investigations of BaTiO₃ ceramics with

- Ba/Ti contents under influence of temperature, *Solid State Ionics*, 303 (2017) 16–23.
- [5] G. Alvarez, A. Conde-Gallardo, H. Montiel, R. Zamorano, About room temperature ferromagnetic behavior in BaTiO₃ perovskite, *Journal of Magnetism and Magnetic Materials* 401 (2016) 196–199.
- [6] Sea-Fue Wang, Yung-Fu Hsu, Yu-Wen Hung and Yi-Xin Liu, Effect of Ta₂O₅ and Nb₂O₅ Dopants on the Stable Dielectric Properties of BaTiO₃–(Bi_{0.5}Na_{0.5})TiO₃-Based Materials, *Appl. Sci.* 5 (2015), 1221-1234.
- [7] Mengying Liu, HuaHao, Weijin Chen, Dongdong Zhou, Millicent Appiah, Binzhi Liu, Minghe Cao, Zhonghua Yao, Hanxing Liu, Zishan Zhang, Preparation and dielectric properties of X9R core-shell BaTiO₃ ceramics coated by BiAlO₃–BaTiO₃, *Ceramics International* 42 (2016) 379–387.
- [8] E. Brzozowski and M.S. Castro, Grain growth control in Nb-doped BaTiO₃, *J. Mater. Process. Technol.*, 168 (2005) 464–470.
- [9] D.-Y. Lu and S-Z. Cui, Defects characterization of Dy-doped BaTiO₃ ceramics via electron paramagnetic resonance, *J. of the European Ceramic Society*, 34(2014) 2217–2227.
- [10] F. Yang, S. Lin, L. Yang, J. Liao, Y. Chen and C.Z. Wang, First-principles investigation of metal-doped cubic BaTiO₃, *Materials Research Bulletin*, Available online 14 March 2017, In Press, Corrected Proof.
- [11] D-Y.Lu, X-Y. Sun and M. Toda, A novel high-k ‘Y5V’ barium titanate ceramics co-doped with lanthanum and cerium, *Journal of Physics and Chemistry of Solids*, 68 (2007) 650–664.
- [12] P. Murugaraj and T.R.N. Kutty, EPR studies on donor doped BaTiO₃ grain boundary layer ceramic dielectrics, *Mat. Res. Bull.*, 20 (1985) 1473-1482.
- [13] Xiang Wang, Min Gu, Bin Yang, Shining Zhu and Wenwu Cao, Hall effect and dielectric properties of Mn-doped barium titanate, *Microelectronic Engineering*, 66 (2003) 855–859.
- [14] E. Brzozowski and M.S. Castro, Influence of Nb⁵⁺ and Sb³⁺ dopants on the defect profile, PTCR effect and GBBL characteristic s of BaTiO₃ ceramics, *Journal of the European Ceramic Society*, 24 (2004) 2499–2507.
- [15] M.M. Vijatovic, B.D. Stojanovic, J.D. Bobic, T. Ramoska and P. Bowen, Properties of lanthanum doped BaTiO₃ produced from nanopowders, *Ceramics International*, 36 (2010) 1817–1824.
- [16] D.-Y. Lu, X.-Y. Sun, B. Liu, J.-L. Zhang and T. Ogata, Structural and dielectric properties, electron paramagnetic resonance, and defect chemistry of Pr-doped BaTiO₃ ceramics, *J. of Alloys and Compounds*, 615(2014) 25–34.
- [17] D.-Y. Lu, Y.-Y. Peng, X.-Y. Yu, X.-Y. Sun, Dielectric properties and defect chemistry of La and Tb co-doped BaTiO₃ ceramics, *J. of Alloys and Compounds* 681 (2016) 128-138.
- [18] F. Yang, S. Lin, L. Yang, J. Liao, Y. Chen and C.Z. Wang, First-principles investigation of metal-doped cubic BaTiO₃, *Materials Research Bulletin*, Available online 14 March 2017, In Press, Corrected Proof.
- [19] W. Sakamoto, K. Noritake, H. Ichikawa, K. Hayashi, T. Yogo, Fabrication and properties of nonreducible lead-free piezoelectric Mn-doped (Ba,Ca)TiO₃ ceramics, *Ceramics International*, 43, Supplement 1, (2017), S166-S171.
- [20] A. Elbasset, L. Mrharrab, S. Sayouri, Dielectric Properties of Ytterbium Yb²⁺ Substituted Barium Titanate Synthesized by Sol-gel Method, *JMES*, 8 (2) (2017), 520-525.
- [21] T. Kolodiaznyh and A. Petric, Analysis of point defects in polycrystalline BaTiO₃ by electron paramagnetic resonance, *J. Phys. Chem. Solids*, 64 (2003) 953–966.
- [22] T.D. Dunbar, W.L. Warren, B.A. Tuttle, C.A. Randall and Y. Tsur, Electron Paramagnetic Resonance Investigations of Lanthanide-Doped Barium Titanate: Dopant Site Occupancy, *J. Phys. Chem. B* 2004, 108, 908-917.
- [23] M.S. Castro, W. Salgueiro and A. Somoza, Electron paramagnetic resonance and positron annihilation study of the compensation mechanisms in donor-doped BaTiO₃ ceramics, *J. of Physics and Chemistry of Solids*, 68 (2007) 1315–1323.
- [24] A. Outzourhit, M.A. El IdrissiRaghni, M.L. Hafid, F. Bensamka and A. Outzourhit, Characterization of hydrothermally prepared BaTi_{1-x}Zr_xO₃, *J. of Alloys and Compounds*, (2002) 214–219.
- [25] N.H. Chan and D.M. Smyth, Defect chemistry of donor-doped BaTiO₃, *J. Am. Ceram. Soc.* 67 (1984) 285–288.
- [26] Mi-Nyeong Lee and Yoon-Chang Park, Dielectric Properties and an EPR Study of Cu- or Zr- Doped BaTiO₃ Ceramics, *Bull. Korean Chem. Soc.*, 16 (1995) 908-911.
- [27] F.D. Morrison, A.M. Coats, D.C. Sinclair and A. West, Charge Compensation Mechanisms in La-Doped BaTiO₃, *J. Electroceramics*. 6 (2001) 219–232.
- [28] H.T. Langhammer, T. Müller, R. Böttcher, V. Mueller and H.-P. Abicht, Crystal structure and related properties of copper-doped barium titanate ceramics, *Solid State Sciences* 5 (2003) 965–971.